JOURNAL OF VIROLOGY, Oct. 2004, p. 10685–10694 Vol. 78, No. 19
0022-538X/04/$08.00+0 DOI: 10.1128/JVI.78.19.10685–10694.2004

Nuclear Export of the Nonenveloped Parvovirus Virion Is Directed by an Unordered Protein Signal Exposed on the Capsid Surface‡

Beatriz Maroto,[1]†§ Noelia Valle,[1]† Rainer Saffrich,[2]‖ and José M. Almendral[1]*

Centro de Biología Molecular "Severo Ochoa," Consejo Superior de Investigaciones Científicas, Universidad Autónoma de Madrid, Cantoblanco, Madrid, Spain,[1] and European Molecular Biology Laboratory (EMBL), Heidelberg, Germany[2]

Received 30 March 2004/Accepted 20 May 2004

It is uncertain whether nonenveloped karyophilic virus particles may actively traffic from the nucleus outward. The unordered amino-terminal domain of the VP2 major structural protein (2Nt) of the icosahedral parvovirus minute virus of mice (MVM) is internal in empty capsids, but it is exposed outside of the shell through the fivefold axis of symmetry in virions with an encapsidated single-stranded DNA genome, as well as in empty capsids subjected to a heat-induced structural transition. In productive infections of transformed and normal fibroblasts, mature MVM virions were found to efficiently exit from the nucleus prior to cell lysis, in contrast to the extended nuclear accumulation of empty capsids. Newly formed mutant viruses lacking the three phosphorylated serine residues of 2Nt were hampered in their exit from the human transformed NB324K nucleus, in correspondence with the capacity of 2Nt to drive microinjected phosphorylated heated capsids out of the nucleus. However, in normal mouse A9 fibroblasts, in which the MVM capsid was phosphorylated at similar sites but with a much lower rate, the nuclear exit of virions and microinjected capsids harboring exposed 2Nt required the infection process and was highly sensitive to inhibition of the exportin CRM1 in the absence of a demonstrable interaction. Thus, the MVM virion exits the nucleus by accessing nonconventional export pathways relying on cell physiology that can be intensified by infection but in which the exposure of 2Nt remains essential for transport. The flexible 2Nt nuclear transport signal may illustrate a common structural solution used by nonenveloped spherical viruses to propagate in undamaged host tissues.

Many eukaryotic viruses invade the nucleus to access the cellular replication and transcription machineries that are necessary for their multiplication. A central process in the life cycle of karyophilic viruses is the passage of viral macromolecules across the nuclear pore complex (NPC) (13, 58), a supramolecular structure regulating nuclear-cytoplasmic transport. For nuclear invasion, viruses use the cellular classical and nonclassical protein import routes (73), which are directed in the classical pathway by basic nuclear localization signals (NLS) (26, 57) recognizing soluble transport receptors of the importin family and other cofactors (31, 72; for a review, see reference 38). The exposure of an NLS to interact with importins (27, 44) and the size of the nuclear viruses, which are generally larger than the 25- to 39-nm functional diameter of the NPC central channel for nondeformable cargo (14, 49), imposes in most cases a drastic conformational change or a complete disassembly of the virus structure for genome delivery into the nucleus (53, 66; for a review, see reference 12).

Late in infection, viruses maturing within the nucleus must egress from the infected cell, and it is generally believed that membrane disorganization and cellular lysis follow the nuclear accumulation of virus particles. Nevertheless, the large enveloped herpesvirus capsid buds by wrapping with the two layers of the nuclear membrane (reviewed in reference 39) or by dissolution of the nuclear lamina with recruited cellular kinases (42), and even for nonenveloped viruses with different sizes a release of infectious particles to the culture medium prior to cell degeneration has been reported in some cases (e.g., see references 7, 9, and 52). However, it is unknown whether viruses actively exit the nucleus by nonlytic mechanisms coupled to the transport machinery of the NPC. The export of proteins and RNA through the NPC proceeds by receptor-mediated recognition of nuclear export signals (NES) (24, 45, 72). A main nuclear export receptor (exportin) for a large number of cellular proteins and subviral components (e.g., see references 71 and 74) is the cellular chromosome region maintenance 1 protein (CRM1 or exportin 1) (48, 61), which binds to leucine-rich NESs directing the cargo protein to the export machinery of the NPC (18, 19) in a manner dependent on Ran-GTP (56), though other types of NES can also bind CRM1 (3, 20). This rapid CRM1/exportin 1 pathway of nuclear export can be inhibited by the antifungal antibiotic leptomycin B (LMB) (28). In addition, there are at least five alternative nuclear export receptors functioning in higher eukaryotes that involve signals distinct from the prototypic leucine-rich NES, are resistant to LMB (29, 62; reviewed in reference 36), and are predominantly regulated by protein phosphorylation (25, 46).

To investigate the signals and the mechanism of export of a nonenveloped icosahedral virus from the mammalian nucleus, we selected the autonomous *Minute virus of mice* (MVM) (8) molecular model of the *Parvoviridae*, a family of viruses with a 5-kb single-stranded DNA genome encapsidated in a 25-nm-

* Corresponding author. Mailing address: Centro de Biología Molecular "Severo Ochoa" (CSIC-UAM), Universidad Autónoma de Madrid, Cantoblanco, 28049 Madrid, Spain. Phone: 34-91-4978048. Fax: 34-91-4978087. E-mail: jmalmendral@cbm.uam.es.

† B.M. and N.V. contributed equally to this work.

‡ N.V. and J.M.A. dedicate this paper to the memories of their respective fathers.

§ Present address: The Scripps Research Institute, La Jolla, CA 92037.

‖ Present address: Otto-Meyerhof-Zentrum, 69120 Heidelberg, Germany.

diameter capsid and maturing within the nuclei of proliferative cells (43). MVM is a common mouse pathogen that causes lethal diseases in newborn and immunodeficient mice (4, 54, 60) and that displays an interesting increased cytotoxic multiplication in some human cancer cells (5, 41). The MVM particle is composed of 60 protein subunits (64, 65), about 10 copies of which correspond to the larger VP1 protein (83 kDa) and the rest of which correspond to the major VP2 protein (63 kDa). During the course of infection, the VP proteins are transported to the nucleus by a nonconventional nuclear localization motif (NLM) localized in the common region of both polypeptides and a consensus NLS mapped at the VP1-specific N-terminal sequence (32, 33, 69), with the latter being also required for the incoming virion to initiate infection (33). The identical fold of the VP1 and VP2 capsid subunits results in characteristic features of the surface (68), such as a cylindrical projection encircled by a canyon-like depression that surrounds the fivefold symmetry axes and a spike-like protrusion in the threefold axes. The VP1 and VP2 N termini are not resolved in the crystal structure of the parvovirus capsid, and for MVM the order is lost at residue 40 (1). Interestingly, the cylinder harbors a pore with a minimum diameter of 8 Å that traverses the capsid shell and contains in virions, but not in empty capsids, weak X-ray-dense material that was modeled as the glycine-rich N-terminal region of one VP2 subunit per channel being projected outside of the virus particle (1, 68).

The unordered VP2 N-terminal domain (2Nt) of some capsid subunits is indeed accessible to proteases and antibodies in DNA-filled virions, but not in either empty native capsids made of VP1 and VP2 that are produced in large amounts in infected cells (50, 65) or VP2-only empty virus-like particles (VLPs) showing identical structural and biophysical properties (23). However, a specific exposure of 2Nt outside of the capsid shell can be induced in both types of empty MVM particles if they are subjected to a heat treatment (23), correlating with a reversible conformational transition detectable by fluorescence (6). In the pathway of viral entry into the host cell, a variable number of VP2 subunits are cleaved by cell proteases at or close to arginine residues 16 and 19 of the exposed 2Nt (8, 50) to form the VP3 (61 kDa) protein, accounting for the varied amounts of VP3 found in viral preparations harvested at late times of infection (64). The VP2 protein subunits of MVM capsids assembled in transformed cells harbored a complex phosphorylation pattern in which the three phosphoserines at positions 2, 6, and 10 of 2Nt formed the most phosphorylated domain of the particle (37), a feature not seen in VLPs (E. Hernando, N. Valle, B. Maroto, and J. M. Almendral, submitted for publication). Furthermore, 2Nt is an immunogenic domain that is likely involved in an important process of the infection, since it elicits neutralizing antibodies and host protection (30).

In this report, we show that 2Nt is a crucial signal for nuclear exit of the DNA-filled mature MVM virus. The degree of 2Nt phosphorylation in two permissive cell types determined the main export route accessed by the virus. In human transformed cells, a high level of 2Nt phosphorylation was important for the NES activity of 2Nt, whereas in normal mouse fibroblasts a poorly phosphorylated 2Nt restricted virus nuclear export to a route that depended on the CRM1 activity in the infected cell. This is the first characterization of a peptide sequence specifically driving an icosahedral nonenveloped virus particle outward from the mammalian nucleus.

MATERIALS AND METHODS

Cell cultures. The A9 ouab^{r}11 mouse fibroblast cell line (A9) and the NB324K simian virus 40-transformed human newborn kidney cell line (324K) were routinely maintained with a minimal number of passages in Dulbecco's modified Eagle medium (DMEM) supplemented with 5% heat-inactivated fetal calf serum (FCS; Gibco BRL). These are reference cell lines that have been described as productive hosts for the MVM parvovirus (63). Cells were synchronized at the G_1/S border by a double block of isoleucine deprivation and aphidicolin treatment (5 μg/ml for 14 h) as described previously (8) or, when indicated, the 324K transformed cells were arrested in G_0 and cultured to confluence (E. Hernando and J. M. Almendral, unpublished data).

For subcellular fractionation, washed cell monolayers scraped into cold phosphate-buffered saline (PBS) were centrifuged and resuspended in hypotonic buffer (1 mM $MgCl_2$, 250 μM $CaCl_2$, 20 mM Tris-HCl [pH 7.5], 0.5% NP-40) on ice for 10 min. The cells were disrupted with a 26-gauge needle with careful microscopic inspection and centrifuged for 5 min at 2,500 rpm and 4°C in a microcentrifuge (Eppendorf 5417R), and the supernatant was taken as the cytoplasmic fraction. The pellet was washed and disrupted once more in the same buffer and finally resuspended as the nuclear fraction. The drug LMB, dispensed into small aliquots under an atmosphere of nitrogen and stored at −20°C in the dark, was used at a concentration of 50 ng/ml (A9) or 100 ng/ml (324K) to inhibit the CRM1-dependent nuclear export pathway (19).

Viruses. Stocks of the prototype strain (wild type [wt]) of the autonomous parvovirus MVMp (11) and of an engineered MVMp mutant lacking phosphorylation at serine positions 2, 6, and 10 of 2Nt (37) (renamed the S/G mutant for this study) were prepared by electroporation of 324K cells with the corresponding infectious plasmids, culturing under conditions that minimized the emergence of secondary mutations (37), and the removal of empty capsids by centrifugation to equilibrium in a CsCl gradient (60). Infectivity titers in 324K cells were determined by a PFU assay or by an infectious unit (IU) assay of VP-expressing cells (fluorescent focus) as described previously (33). The life cycle of MVMp viruses was analyzed in synchronized cells released into the cell cycle upon infection (multiplicity of infection, 1 to 5 PFU/cell in PBS) by either removal of the aphidicolin blockade (A9 and 324K cells) or subculturing by 4 h postinfection (hpi) at a density of 7,000 cells/cm^2 (324K cells).

Analysis of radiolabeled viral particles. Cells seeded at a density of 10,000 cells/cm^2 in 90-mm-diameter dishes were cultured overnight, infected, and labeled at the indicated times in methionine-free DMEM supplemented with 10% normal medium, 10% dialyzed FCS, and 200 μCi of [^{35}S]methionine-cysteine (SJ5050; Amersham)/ml or starved for 4 h in phosphate-free DMEM–10% dialyzed FCS and labeled in the same medium with 1 mCi of carrier-free [^{32}P]orthophosphate (PBS13; Amersham)/ml. For the purification of labeled viral particles, cultures were harvested at either an early (22 hpi) or late (48 hpi) time postinfection and processed according to previously described procedures (37, 59). After centrifugation to equilibrium in a CsCl gradient, fractions containing labeled particles with a density corresponding to empty MVM capsids (1.32 g/ml) and DNA-filled virions (1.39 to 1.41 g/ml) were pooled and extensively dialyzed against PBS. ^{32}P-labeled gel-isolated VP2 proteins from immunoprecipitates or purified empty capsids were subjected to two-dimensional tryptic phosphopeptide analysis by digestion with *N*-tosyl-L-phenylalanine chloromethyl ketone–trypsin (sequencing grade; Boehringer) and resolution in 20- by 20-cm thin-layer chromatography plates (Merck, Darmstadt, Germany) performed according to previously reported methods (2, 37). The plates were exposed to a radioanalytic imaging system (Fujix BAS 1000; Fuji).

Purification of MVM particles and 2Nt exposure. MVMp empty capsids containing the VP1 and VP2 structural proteins, produced in 324K cells, and VP2-only VLPs, produced in insect cells with a baculovirus system, were purified by centrifugation through a sucrose gradient and by centrifugation to equilibrium in a CsCl gradient as previously described (23). The particles were subjected to a moderate heat treatment at 50°C for 10 min in PBS to induce the conformational transition that specifically externalizes 2Nt (6, 23) and then were kept frozen at −70°C until microinjection.

Preparation of BSA-peptide conjugates. Two peptides with the sequence MSDGTSQPDSGNAVHC, corresponding to the first 16 amino acids of the VP2 N terminus either harboring phosphorylated serines at positions 2, 6, and 10 (2Nt) or without phosphorylated residues [2Nt(−p)], were synthesized on an Applied Biosystems model 431A peptide synthesizer by Fast Moc chemistry and were purified by reverse-phase high-pressure liquid chromatography. The synthetic peptides were coupled to bovine serum albumin (BSA) by use of the

bifunctional cross-linking reagent sulfo-SMCC (Pierce Chemical). BSA (2 mg) (Boehringer Mannheim) was dissolved in 400 μl of PBS (pH 7.4) and incubated for 1 h at 20°C with 3.2 mg of sulfo-SMCC. BSA was subsequently separated from the unreacted sulfo-SMCC by chromatography through a Sephadex G-25 NAP-10 column (Pharmacia), mixed with 1 mg of peptide dissolved in 1 ml of PBS, and incubated at 4°C overnight with gentle rotation. Conjugation was assessed by sodium dodecyl sulfate–10% polyacrylamide gel electrophoresis (SDS–10% PAGE) analysis, and BSA-peptide conjugates were subsequently purified in a Sephadex G25 NAP-10 column and concentrated to 2 mg/ml in a Minicon 30 concentrator (Amicon).

Microinjection of somatic cells. A9 and 324K cells were seeded at a density of 3×10^4 cells/cm^2 on 12-mm-diameter gridded glass coverslips (Cellocate; square size, 175 μm; Eppendorf) in DMEM supplemented with 10% FCS, and then the cells were synchronized and infected as described above, when required. Selected fields of 80 to 100 cells were microinjected intranuclearly with an automated injection system (Compiclnject; Cell Biology Trading, Hamburg, Germany). Injections were done with 20 to 50 fl per cell with purified preparations of MVM empty capsids (approximately 10^4 particles/cell) or BSA-peptide conjugates (approximately 4×10^5 molecules/cell), together with fluorescein isothiocyanate (FITC)-dextran 70 (Molecular Probes, Leiden, The Netherlands) to monitor injection and nuclear membrane integrity. The cells were extensively washed in PBS, fixed at the indicated hours postinjection with 4% paraformaldehyde for 5 min at room temperature, and further permeabilized with methanol-acetone (1:1) at −20°C for 7 min before being stained with antibodies. A qualitative score of the immunofluorescence (IF) phenotype was determined for every healthy cell showing an intact nuclear membrane (approximately 75% of the injected cells).

Antibodies. A polyclonal antiserum against the VP2 N-terminal domain (α-2Nt antiserum) was raised in a rabbit and used at a 1/200 dilution. The chemically synthesized 2Nt peptide mentioned above was activated and covalently coupled in an excess molar ratio to keyhole limpet hemocyanin (Pierce) with the heterobifunctional cross-linker *m*-maleimidobenzoyl-*N*-hydroxysuccinimide as described previously (32), extensively dialyzed against PBS, and injected subcutaneously, emulsified in Freund's adjuvant, at 200 μg per dose. This antibody recognized similarly the 2Nt and 2Nt(−p) peptides in an enzyme-linked immunoassay (not shown). Capsid polyclonal antisera raised in rabbits against purified MVM empty particles (α-CAP antiserum) (59) and against denatured VP2 isolated from gels (α-VPs) (Hernando and Almendral, unpublished data) were used at a 1/200 dilution. For the specific recognition of assembled particles, a B7 monoclonal antibody (capsid MAb) recognizing an epitope conformed at the MVM capsid surface (34) was used at a 1/40 dilution. Viral gene expression in infected cells was monitored with a MAb recognizing the major nonstructural protein NS1 (60). A rabbit anti-human CRM1 serum (α-CRM1) (18) was used at a 1/100 dilution, and a MAb against BSA (α-BSA) (clone BSA-33; Sigma) was used at a 1/20 dilution.

Immunological analyses. For indirect IF, cells seeded onto glass coverslips were fixed in methanol-acetone (1:1) at −20°C for 7 min and then incubated with the indicated primary antibodies diluted in PBS supplemented with 5% horse serum. Bound immunoglobulin G (IgG) was visualized with secondary antibodies (Jackson Immunoresearch Laboratories, Inc.), generally diluted 1/200, including a goat anti-rabbit antibody conjugated to Texas red, a goat anti-mouse antibody conjugated to FITC, and a donkey anti-mouse antibody conjugated to indodicarbocyanine (Cy5). Confocal microscopy was performed with a Radiance 2000 system (Bio-Rad) coupled to an Axiovert S100 TV fluorescence microscope (Zeiss). Samples were examined with lasers giving excitation lines at 488 nm (FITC, filter HQ 500-530), 638 nm (Cy5, filter HQ 660 LP), and 543 nm (Texas red, filter HQ 600 LP or filter HQ 575-625 for triple labeling). Data from the channels were collected sequentially at a resolution of 1,024 by 1,024 pixels, using optical slices with thicknesses between 0.5 and 1 μm. For immunoprecipitation, the samples were adjusted with a buffer containing 150 mM NaCl, 50 mM Tris (pH 8.0), 0.3% SDS, 1% NP-40, and 0.75% 2-mercaptoethanol and with protease and phosphatase inhibitors (1 mM phenylmethylsulfonyl fluoride, 10 μg of aprotinin/ml, 10 μg of pepstatin/ml, 10 μg of leupeptin/ml, 5 mM NaF, 20 mM β-glycerophosphate). Homogenates were incubated overnight at 4°C with the indicated antisera, and the immune complexes were precipitated with protein A-Sepharose (10% [wt/vol]) and washed with a mixture containing cold PBS, 0.05% NP-40, and 1% BSA. Bound proteins were eluted by heating the samples for 5 min at 95°C in Laemmli buffer and were subjected to SDS-PAGE. The gels were fixed, dried, and exposed for autoradiography in a phosphorimager (Fujix Bas 1000).

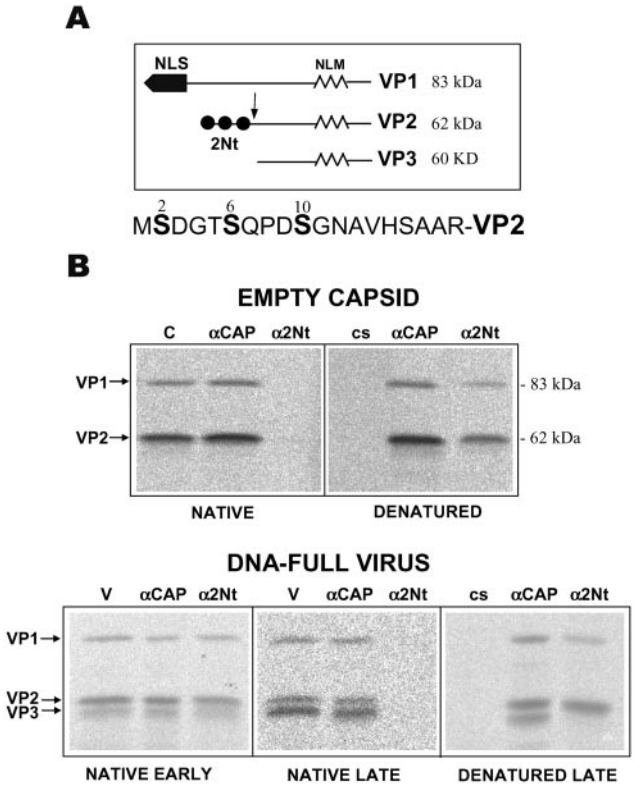

FIG. 1. Exposure of 2Nt in MVM capsid and virus. (A) Transport sequences in MVM structural proteins. Shown are the NLM (residues 670 to 680 of VP1) in the common sequence of the three polypeptides and the NLS of VP1 (residues 6 to 10 and 87 to 90) (33). The phosphoserine residues at positions 2, 6, and 10 of VP2 (black balls) within 2Nt and the approximate VP2 processing site to produce VP3 (arrow) are indicated. The entire 2Nt amino acid sequence of the prototype MVM strain is shown below. (B) Immunological analysis of 2Nt exposure. ^{35}S-labeled empty capsids (C) and DNA-filled virus (V) were purified from 324K cultures early (22 hpi) and late (48 hpi) in the infection and subsequently were immunoprecipitated as either native or denatured (boiled for 5 min in 0.2% SDS) proteins with the polyclonal α-CAP antiserum, the α-2Nt antiserum, or a control preimmune serum (cs). The positions of the virus structural proteins in the SDS–10% PAGE gels are indicated to the left.

RESULTS

An exposed 2Nt is required for nuclear exit of mature MVM virus. The 2Nt is contained within the sequence of the two structural polypeptides of MVM (Fig. 1A). To investigate the role of 2Nt in the late steps of the MVM life cycle, we assessed the specificity of a polyclonal antiserum raised against the 2Nt peptide sequence (α-2Nt antiserum) by using purified viral particles (Fig. 1B). The VP2 and VP1 proteins were recognized by α-2Nt only upon heat denaturation of the capsids (Fig. 1B, top panel), in agreement with the internal disposition of the N termini of the VP subunits in empty MVM particles (10, 23). In contrast, DNA-filled viruses harvested at early times prior to the reinfection of cells, with most VP2 subunits still unprocessed, were efficiently immunoprecipitated in their native state with α-2Nt (Fig. 1B, bottom panel). Viruses harvested at late times from infected cultures and harboring a large proportion of VP2 subunits cleaved to form VP3 (presumably those ac-

cessed by cellular proteases outside of the capsid shell) could not be immunoprecipitated in their native form by α-2Nt, but their VP1 and VP2 subunits were quantitatively immunoprecipitated if the particles were disassembled by heat denaturation prior to the α-2Nt reaction (Fig. 1B, bottom panel). Thus, α-2Nt is a specific antibody for the immune recognition of DNA-filled MVM virions that are newly formed in infected cells.

MVM maturation in a single infection cycle was analyzed with the 2Nt antiserum in combination with a MAb reacting against the intact capsid (capsid MAb) (34). The assembly of MVM empty capsids exclusively reacting with the capsid MAb antibody (Fig. 2A, top row) was first detected in the nuclei of synchronously infected 324K fibroblasts around 18 hpi. As the infection progressed (22 hpi), the detection of DNA-filled particles showing α-2Nt reactivity marked the onset of virus maturation. By 24 hpi, while empty capsids remained in the nucleus, staining by the α-2Nt serum became either weak or undetectable in most infected cells, indicating a specific nuclear egress of the mature DNA-filled virions. This phenomenon could not be inhibited by high doses of LMB added to the culture, suggesting that the CRM1 transport factor does not play an essential role in the nuclear export of MVM virions in transformed 324K fibroblasts (Fig. 2A). Later in the infection cycle, the cytoplasm of most infected cells was stained with the capsid MAb antibody (not shown), a phenomenon that was indirectly related to the activity of the NS2 nonstructural protein (15, 40), which is described elsewhere (35). The distinct subcellular distribution of the newly formed empty capsids and DNA-filled virions in the MVM infection was further examined by equilibrium centrifugation of ^{35}S-labeled particles harvested from synchronized cells (Fig. 2B). Virions and empty capsids were demonstrable mostly in the nuclear fraction at 22 hpi, but at 24 hpi most virions were recovered in the cytoplasmic fraction while empty capsids still remained in the nucleus. Therefore, we concluded that DNA-filled virions, but not MVM empty capsids, may actively exit the nuclei of permissive cells soon after maturation and prior to nuclear membrane disruption.

Phosphorylated 2Nt functions as an NES for MVM capsids in transformed cells. The protein subunits forming the MVM capsid harbor a high level of 2Nt phosphorylation in serine residues at positions 2, 6, and 10 of VP2 (Fig. 1A) (37). To study whether the phosphorylated residues of 2Nt play any role in virion nuclear export, we similarly analyzed the kinetics of maturation of the S/G mutant lacking these phosphorylatable serines (37). A high level of nuclear accumulation of S/G empty capsids and DNA-filled virions could be demonstrated, with a time course comparable to that of the wt (Fig. 2A, bottom panels). However, at the time the wt virions had completed their nuclear exit (24 hpi), the S/G virions remained accumulated within the nucleus, giving a punctate signal that was predominantly localized in the nuclear periphery (Fig. 2A, bottom panels and insets). This result indicated that the lack of 2Nt phosphorylation hampered translocation of the S/G virion through the NPC, although its docking to the inner nuclear membrane may have been unaffected. The phenotype of nuclear retention of the S/G virions was further supported by the subcellular distribution of maturing infectious virions (Fig. 2C). Intracellular S/G infectious viruses accumulated during

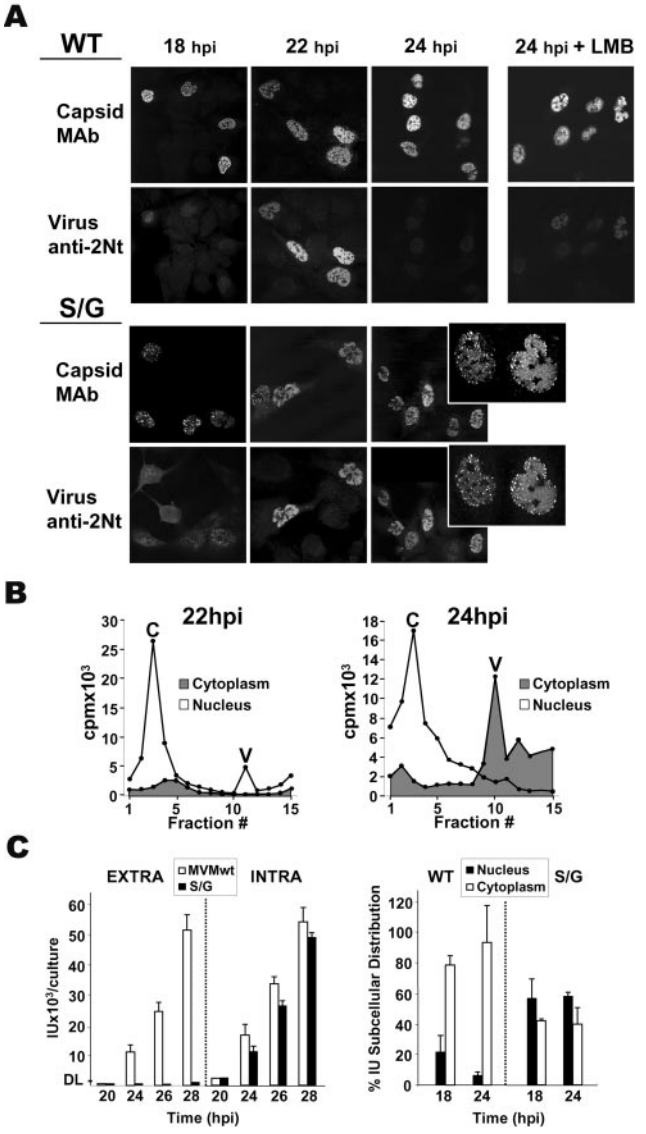

FIG. 2. 2Nt phosphorylation is important for nuclear exit of infectious virus in transformed cells. (A) Subcellular localization of MVMp particles in a single round of infection of transformed 324K cells synchronized by growth to confluence. Shown are representative fields of cells visualized by confocal microscopy and stained with the MVM-capsid MAb and the α-2Nt antibody specific for DNA-filled virions. +LMB, wt particles at 24 hpi in cells treated with LMB (100 ng/ml) from 14 hpi. Insets, intranuclear punctate phenotype of S/G particles. (B) Subcellular distribution of newly formed MVM particles. Infected synchronous cells were labeled with ^{35}S since 6 hpi, and wt viral particles harvested from fractionated cells at the indicated times were sedimented through a sucrose cushion and centrifuged to equilibrium in a CsCl gradient. A representative result of ^{35}S cpm distribution in the banding positions of the empty capsids (c) and DNA-filled virions (v) is shown. (C) The S/G phosphorylation mutant shows a defect in nuclear egress. (Left) Infectious units (IU) of wt and S/G viruses in the culture medium (extra) and inside the cells (intra) at the indicated postinfection times for synchronized 324K cells. DL, detection limit of the assay. (Right) Percentage of subcellular distribution of infectious viruses in fractionated cells. Data are means and standard errors from three independent experiments.

the course of the infection at a similar rate to that of the wt, but while the extracellular wt virus increased proportionally to the intracellular level, the infectious S/G virus was blocked from exiting the cells (Fig. 2C, left panel). Inside the cells, wt infectious virions were detected mainly in the cytoplasm late in the infection, in contrast to the relative nuclear retention of the S/G virions (Fig. 2C, right panel). These results indicated hampered nuclear export of the S/G mutant virus in transformed cells.

The nuclear retention of the S/G virus led us to hypothesize that 2Nt could act in its phosphorylation configuration as a nonconventional NES for the viral capsid in transformed cells. To directly test this hypothesis, we microinjected highly purified MVMp empty particles harboring phosphorylated or nonphosphorylated 2Nt into the nuclei of 324K cells. The particles used were empty capsids obtained from MVMp-infected 324K cells which were phosphorylated at the serine residues of 2Nt (37) and VLPs obtained from insect cells, which were structurally indistinguishable (23) but nonphosphorylated (Hernando et al., submitted). The purified particles were subjected to moderate heat, which specifically externalizes the 2Nt sequence out of the protein shell (6, 23), mimicking the configuration found in DNA-filled virions (51, 65). The native (C, VLP) and heated (Ch, VLPh) viral particles illustrated in Fig. 3A were microinjected into the nuclei of 324K cells, and their subcellular distribution was analyzed either immediately (0 h) or at 1 h postinjection. Both native particles remained quantitatively inside the nucleus at 1 h postinjection (Fig. 3B, left panels). However, particles subjected to heat behaved differently (Fig. 3B, right panels), as control heated capsids could be stained within the nucleus soon after injection (0 h) but became virtually undetectable after 1 h of incubation, in contrast to the evident nuclear retention of the nonphosphorylated heated VLP particles. To gain further support for a direct role of phosphorylated 2Nt in capsid transport during natural viral infections, we analyzed the subcellular distribution of microinjected capsids in MVMp-infected 324K cells. Infected cells (2 PFU/cell) synchronized by a double block (see Materials and Methods) were injected at 6 h post-aphidicolin release to avoid interference with endogenous capsid assembly, the onset of which is detectable several hours later in the infection cycle (Fig. 2) (35). Native empty capsids (C) remained in the nuclei of injected cells for 1 h, even under patent ongoing infection, denoted by staining for de novo synthesized NS1 major nonstructural protein (Fig. 3B, bottom panels). In contrast, as shown above, heated capsids (Ch) became either weakly detectable or nondetectable in injected cells after 1 h of incubation, regardless of NS1 expression. In summary, microinjected viral particles used 2Nt in its phosphorylated configuration as the driving sequence for nuclear export of the MVM capsid.

The NES activity of 2Nt was further evaluated in protein conjugates composed of a chemically synthesized phosphorylated 2Nt peptide or its nonphosphorylated peptide counterpart [2Nt(−p)] coupled to BSA and microinjected into the nuclei of 324K cells (Fig. 3C). The nonphosphorylated conjugate protein remained in the nuclear compartment even at late times postinjection, in contrast to the partial but general nuclear export of BSA promoted by the phosphorylated 2Nt peptide at several hours postinjection. A mixed nuclear-cytoplasmic staining for the 2Nt-BSA conjugate in the population

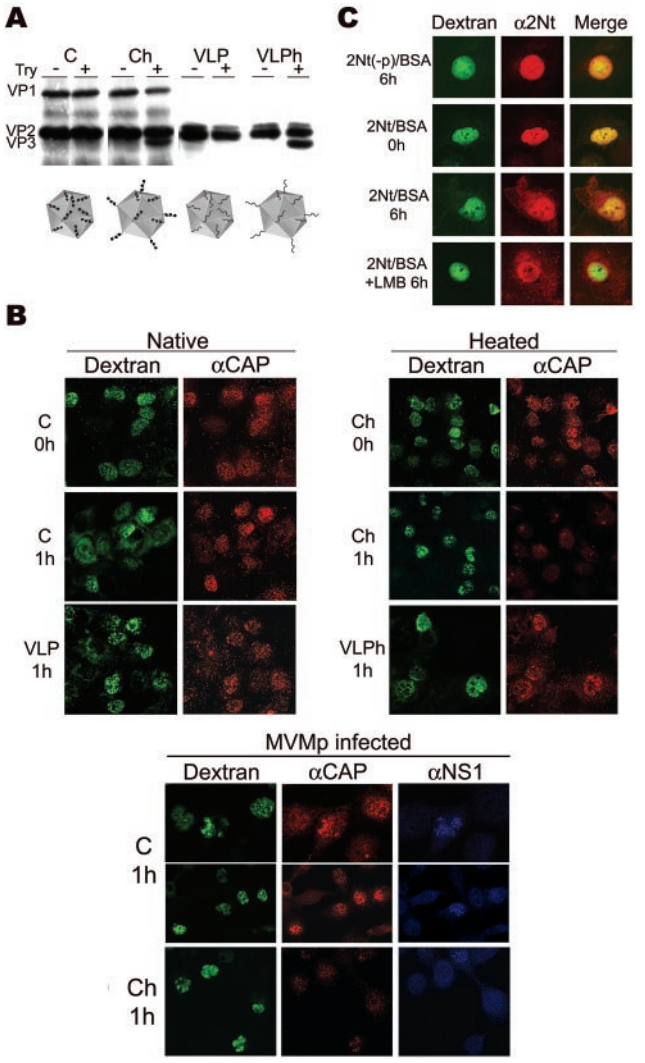

FIG. 3. Nuclear export activity of 2Nt in transformed cells. (A) Heat-triggered exposure of 2Nt in MVM particles. Purified native empty capsids (C) and VLPs or the respective particles heated at 50°C for 10 min (Ch and VLPh) were tested for 2Nt exposure by trypsin (Try) digestion (23), and the cleavage of VP2 to form VP3 was visualized by immunoblotting with an α-VP antiserum. The four types of microinjected particles, with phosphorylated serine residues of 2Nt in natural capsids (black balls) or no phosphorylation in VLPs, are illustrated at the bottom. (B) Subcellular localization of MVM particles injected inside the 324K nucleus. Viral particles were injected with dextran-FITC in noninfected (upper panels) or infected (lower panels) cells and analyzed either immediately (0 h) or at 1 h postinjection by confocal laser microscopy after staining with the α-CAP serum and the α-NS1 MAb antibody where indicated. Shown are representative fields at different magnifications with clusters of injected cells and FITC-dextran marking intact nuclear membranes. (C) Confocal analysis of 2Nt(−p)-BSA and 2Nt-BSA protein conjugates microinjected into the 324K nucleus. Cells were fixed at the indicated times postinjection and stained with the α-2Nt antibody. Where indicated (+LMB), LMB (100 ng/ml) was added to the cultures after injection.

of injected cells was also observed in the presence of a high concentration of LMB (Fig. 3C, bottom). The results of this experiment further support the function of phosphorylated 2Nt as an NES that is not strictly dependent on CRM1 in transformed cells.

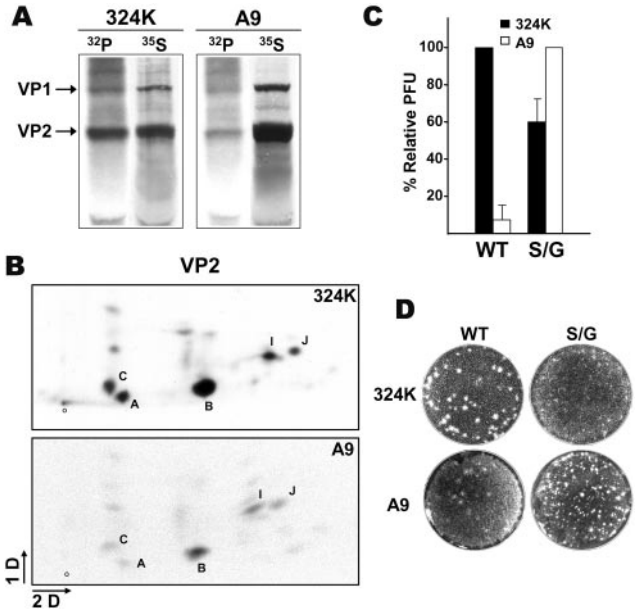

FIG. 4. Cell-type-dependent 2Nt phosphorylation and MVM infection. (A) Quantitative analysis of MVM capsid phosphorylation in permissive cells. The respective cultures (10^6 cells) were infected with MVMp (5 PFU/cell) and labeled in parallel at 2 hpi with [^{35}S]Met-Cys (^{35}S) or [^{32}P]orthophosphate (^{32}P). Capsid proteins were immunoprecipitated at 20 hpi with the α-VP antiserum from identical amounts of boiled homogenates and were resolved by SDS–10% PAGE. (B) Two-dimensional phosphopeptide map of VP2 capsid subunits. The VP2 protein purified from the gels was digested with trypsin and subjected to two-dimensional TLC analysis. The plates were exposed to autoradiography for 5 days with an intensifying screen at −70°C. Peptide B, corresponding to 2Nt, and other main phosphopeptides are designated as described previously (37). 1D, first dimension; 2D, second dimension; O, origin. (C) Plaque-forming capacity of wt and S/G viruses. Identical numbers (IU) of gradient-purified viruses were added to the respective cell monolayers, and the infectivity was scored as the percentage of PFU with respect to the most permissive cell for each virus. The figure outlines the averages and standard errors from three independent determinations. (D) Representative result illustrating the ratio and morphology of virus plaques in the reference cell lines.

MVM capsid phosphorylation is important for infection in a cell-type-dependent manner. To investigate MVMp nuclear exit in permissive nontransformed cells, we comparatively studied capsid phosphorylation and viral plaque-forming capacities in the two cell lines that are commonly used to grow this virus, transformed 324K cells and A9 normal mouse fibroblasts (63). The degree of VP1 and VP2 capsid protein phosphorylation was determined by paralleled [^{35}S]Met-Cys and [^{32}P]orthophosphate labeling in both cell types. As shown in Fig. 4A, the virus structural proteins that accumulated in 324K cells harbored a severalfold higher phosphorylation level than those in A9 cells. Moreover, tryptic phosphopeptide maps of the VP2 subunits assembled in gradient-purified MVMp particles showed the previously reported characteristic two-dimensional phosphorylation pattern (37), in which phosphopeptide B, which corresponds to 2Nt, harbored most of the ^{32}P label (Fig. 4B). Therefore, MVMp capsids produced in the two permissive cell lines share a similar distribution of phosphorylated residues in the protein subunits, although the degree of occupancy of these sites by phosphate radicals, including the sites in the 2Nt sequence, is significantly higher in transformed 324K cells.

The relationship between 2Nt phosphorylation and MVMp infection was analyzed by comparing the specific infectivity of the wt with that of the S/G virus, whose capsid lacks phosphorylation exclusively at the VP2 N-terminal sequence (37). In agreement with previous reports (21), the plaque-forming capacity of wt MVMp was 10 to 20 times higher in 324K cells than in A9 cells (Fig. 4C), and plaques were larger in the former cells (Fig. 4D). In sharp contrast, the S/G mutant showed a lower plaque-forming capacity in 324K cells than in A9 cells (Fig. 4C), and plaques in A9 cells were clearer than the wt plaques (Fig. 4D). These results demonstrated that 2Nt phosphorylation is an important determinant of MVMp plaque-forming capacity, but the assay used may be influenced by the capacity of viral spreading to neighboring cells. Indeed, the S/G plaque phenotype was in agreement with its above-mentioned defect in nuclear exit and cellular egress in 324K cells (Fig. 2). Interestingly, these results also suggest that the S/G virus may use an alternative route independent of 2Nt phosphorylation to efficiently egress and form plaques in A9 mouse fibroblasts.

MVM virions use a CRM1-dependent pathway to exit the nuclei of mouse fibroblasts. The high infection capacity of the S/G virus in A9 mouse fibroblasts in the absence of 2Nt phosphorylation prompted us to investigate the route of nuclear export of MVM in this cell type. The subcellular distribution of virus particles in a single round of infection of highly synchronized A9 cells was determined by confocal microscopy, with staining with specific antisera (Fig. 5A). The wt and S/G capsids and virions accumulated in the A9 nucleus by 18 hpi, irrespective of the presence or absence of LMB. By 20 hpi, a major loss of nuclear staining for wt DNA-filled virions was consistently noticed in a large proportion of cells, a phenomenon that was even more evident for the S/G virions. Treatment with LMB significantly, but not completely, inhibited nuclear exit of the wt virions. However, the inhibitory effect of LMB was absolute for the export of S/G virions in the entire infected cell population. These data were confirmed by the distribution of infectivity between the nuclear and extranuclear (cytoplasm plus extracellular medium) compartments shown in Fig. 5B, as wt and S/G infectious particles showed an equivalent distribution by 18 hpi and had efficiently exited from the nucleus by 20 hpi. The transport of infectious virus in A9 cells was significantly inhibited by LMB, and particularly the nuclear exit of S/G virions was more sensitive to the addition of the drug, paralleling the findings obtained by IF analysis. We concluded that wt and S/G viruses exit the nuclei of normal mouse fibroblasts mainly by a CRM1-dependent pathway, although the wt virus may partly use an alternative CRM1-independent route with a low efficiency in this cell type.

Nuclear export of MVM virions in mouse fibroblasts requires exposed 2Nt and the infection process. To gain insights into the mechanism regulating the trafficking of MVM virions in A9 fibroblasts, we investigated the nuclear export activity of 2Nt in empty viral capsids. The four types of MVM particles outlined in Fig. 3A were microinjected into the A9 nucleus, and their subcellular distribution was analyzed by confocal microscopy. Unlike the results obtained with 324K cells (Fig. 3B), both native (C, VLP) and heated (Ch, VLPh) viral empty

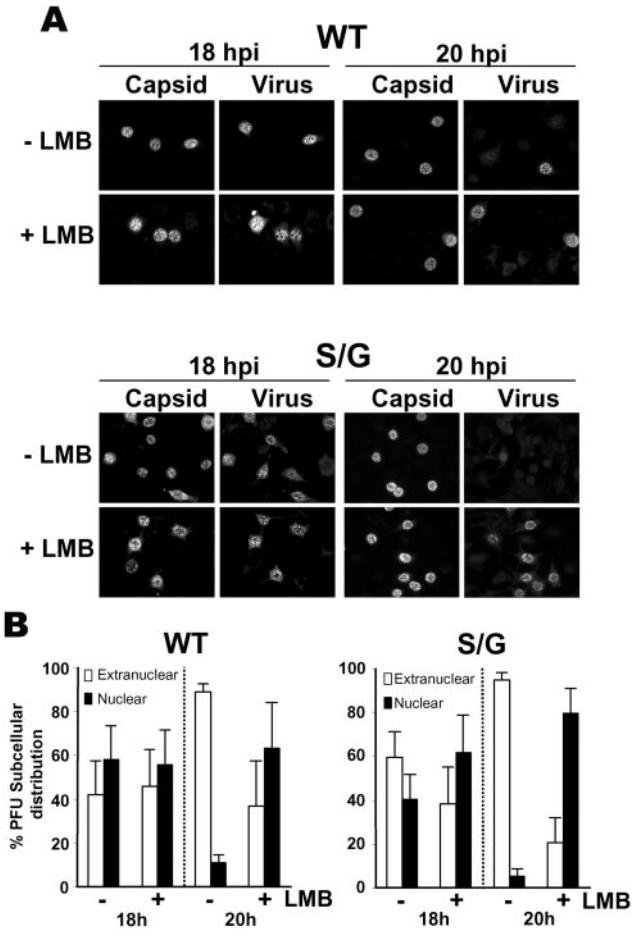

FIG. 5. Nuclear export of MVM virions in A9 mouse fibroblasts. (A) Involvement of CRM1 in MVM exit from the mouse fibroblast nucleus. The panels of cells visualized by confocal microscopy show the subcellular distribution of wt and S/G empty capsids (capsid MAb staining) and DNA-filled virions (α-2Nt staining) that were newly synthesized during the MVM infection cycle in synchronized A9 cells in the presence (+) or absence (−) of LMB. (B) Distribution of infectious virions. Synchronized cells were fractionated at the indicated times postinfection in the absence (−) or presence (+) of LMB, and the percentages of wt and S/G infectious viruses localized inside or outside (cytoplasm plus extracellular medium) the nucleus were determined by a plaque assay.

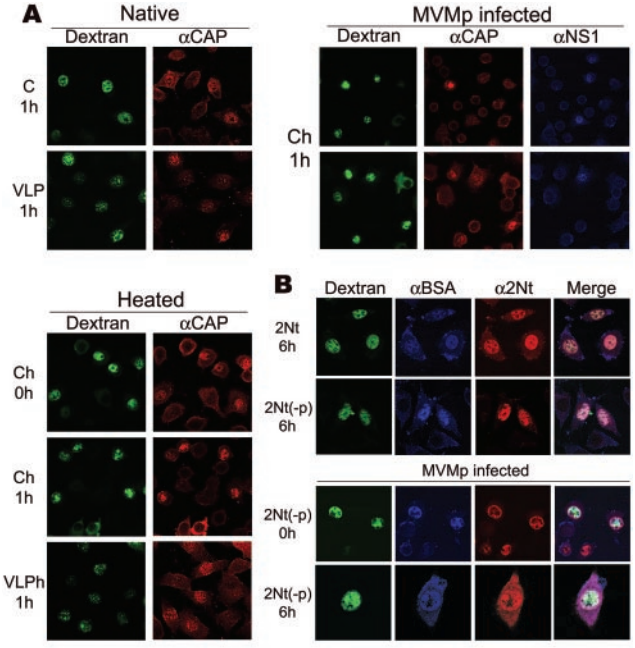

FIG. 6. Analysis of 2Nt export activity in A9 mouse fibroblasts. (A) Transport of MVM particles. The native and heated MVM particles illustrated in Fig. 3A were injected into the nuclei of either growing or synchronized and MVMp-infected (1 PFU/cell) mouse fibroblasts at 6 hpi and then were stained with the α-CAP antiserum. The infection onset in some cells was demonstrated by staining with the α-NS1 antiserum. Representative fields of injected cells (two panels for infection studies) denoting intact nuclear membranes are shown. (B) Transport activity of 2Nt for a heterologous protein. The localization of phosphorylated (2Nt) and unphosphorylated [2Nt(−p)] peptides coupled to BSA and microinjected into the nuclei of uninfected (upper panels) or MVMp-infected (lower panels; injection at 14 hpi) A9 mouse fibroblasts is shown. The subcellular distribution of the conjugates was examined by confocal microscopy with the α-BSA and α-2Nt antisera. Shown are representative cells for each experiment.

particles remained mainly accumulated in the nucleus after 1 h of incubation postinjection (Fig. 6A, left panels). This lack of export activity of nonphosphorylated 2Nt exposed in heated VLPs was unexpected, given the efficient A9 infection by the S/G virus (Fig. 4 and 5), and therefore a hypothetical role of the infection process in nuclear transport of the capsid was analyzed with viral particles injected into highly synchronized MVM-infected cells. Nuclear staining of heated capsids (Ch) in infected cultures was demonstrable at 0 h postinjection (not shown), but upon 1 h of incubation, capsid staining was weakened to background levels or showed a mixed nuclear-cytoplasmic phenotype in a large proportion of cells (Fig. 6A, right panels). Remarkably, this change in the heated capsid subcellular distribution was found only in those cells showing ongoing infection by NS1 expression. Similar results were obtained with heated VLPs injected into infected cells (not shown). These data validated the exposed 2Nt as an NES for intact MVM capsids in infected mouse fibroblasts.

Finally, the export activity of 2Nt in its natural phosphorylated and unphosphorylated [2Nt(−p)] configurations on a heterologous protein in A9 cells was investigated with conjugates coupled to BSA. As shown in Fig. 6B (top panels), both protein conjugates (stained with α-BSA and α-2Nt antibodies) remained in the nucleus for several hours postmicroinjection, indicating that unlike the results obtained with transformed 324K cells (Fig. 3), phosphorylation was not sufficient for 2Nt to act as an NES in A9 mouse fibroblasts. Yet a preliminary transport study of the 2Nt(−p)-BSA conjugate attempted in infected nonsynchronous A9 cells showed a mixed nuclear-cytoplasmic pattern of BSA distribution in a small but significant number of cells (Fig. 6B, bottom panel), suggesting that a factor induced during MVMp infection may confer nuclear export activity to 2Nt in mouse fibroblasts.

DISCUSSION

Signals and routes for MVM nuclear exit. This report describes the signal for active nuclear export of a nonenveloped icosahedral virus, the parvovirus MVM, infecting permissive

fibroblasts at different physiological stages. The efficient exit of mature viral particles out of the nuclei of infected transformed (324K) and nontransformed (A9) cells was shown to proceed via a short amino acid sequence in the N terminus of the VP2 capsid protein, called 2Nt for this study, which is exposed outside of the shell of virions with an encapsidated genome. Unlike the earlier and rapid nuclear export of mature viruses in 324K and A9 cells, empty capsids lacking 2Nt exposure remained inside the nucleus late in the natural infection (Fig. 2 and 5), as did native empty capsids and VLPs that were microinjected into the nuclei of growing and MVM-infected cells (Fig. 3 and 6). However, microinjected phosphorylated empty capsids exited the nuclei of 324K cells and infected A9 cells if they were previously subjected to a heat-induced structural rearrangement that exposed 2Nt (6, 23), mimicking viral genome encapsidation.

We have identified some features of the export routes that are followed by MVM virions in a cell-type-dependent manner. In infected 324K human transformed cells, the MVM capsid was highly phosphorylated (Fig. 4), and the phosphorylated serine residues of 2Nt were necessary for the transport activity of this sequence by a route for which CRM-1 was apparently not essential (Fig. 2 and 3). This was consistent with the lack of homology of 2Nt with consensus NESs containing abundant leucine residues, which are common substrates of CRM-1 (18, 19), and with previous reports on the regulation of nuclear export by cargo phosphorylation through as yet poorly defined CRM-1-independent pathways (25, 36, 46). The nuclear export of BSA conjugates in 324K cells by the activity of phosphorylated 2Nt (Fig. 3C) was low if compared with the rapid and absolute cytoplasmic phenotype often obtained for microinjected peptides exported via CRM-1 (e.g., see reference 16), suggesting that 2Nt accesses a less powerful transport machinery than those used by abundant cellular cargoes (70). Alternatively, the proper activity of 2Nt may require its exposure in the context of the capsid, as suggested by the significant nuclear export of the approximately 10^4 phosphorylated heated capsids that were microinjected per cell (Fig. 3), which may be sufficient for the export and spreading of the total number of mature viruses produced per cell along the infection cycle. A comprehensive understanding of the export route accessed by phosphorylated 2Nt and the cellular kinase involved in transformed 324K cells may shed light on fundamental aspects of the characteristic parvovirus tropism for neoplastic cells (41).

The major route of nuclear export followed by MVM virions in nontransformed A9 mouse fibroblasts was not related to protein phosphorylation, as judged by the low level of MVM capsid phosphorylation in infected A9 cells (Fig. 4A and B) and by the nuclear accumulation of phosphorylated heated particles that were microinjected into noninfected cells (Fig. 6). Instead, the efficient nuclear export of MVM viruses lacking 2Nt phosphorylation, like that of microinjected heated capsids in A9 cells, proceeded by a route that was sensitive to CRM-1 inhibition and that required the infection process (Fig. 5 and 6). These results may suggest the concourse of a virally induced protein adapter allowing access of the MVM capsid to the CRM1 export route, similar to the transport of some subviral nucleic acid-protein complexes coupled to CRM1 (e.g., see references 16 and 47). Interestingly, efficient MVM capsid release and viral spreading in mouse A9 cells, and to some extent in 324K cells, required the CRM1 interactive domain of the nonstructural NS2 protein (15, 40), and thus NS2 could presumably be the MVM-encoded factor that adapts the capsid and 2Nt to the CRM1 pathway in infected cells. However, extensive immunoprecipitation analyses failed to demonstrate any consistent interaction of the intact MVM capsid or mature virions with either CRM1 or NS2 (data not shown), suggesting an indirect involvement of CRM1 in the transport process.

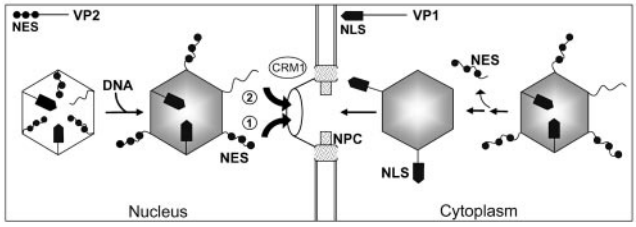

FIG. 7. Signals regulating trafficking of the MVM virus across the nuclear membrane. Cytoplasmic entry events are as follows: cleavage of 2Nt and externalization of the NLS contained in the VP1 N terminus contribute to the docking of the incoming virus to the NPC. Nuclear export events are as follows: the viral structural proteins translocated to the nucleus by import sequences (Fig. 1) assemble first into empty capsids that likely act as intermediates of viral maturation. Genome encapsidation triggers the externalization of 2Nt of some VP2 subunits outside the capsid shell, driving the active export of mature virus. In transformed cells, a high level of capsid phosphorylation endows 2Nt with NES activity (route 1), whereas in normal fibroblasts the lower 2Nt phosphorylation restricts virus nuclear export to a CRM1-dependent mechanism requiring the infection process (route 2).

Further recent experimental evidence not only supports indirect CRM1 involvement in the nuclear egress of MVM particles, but also indicates that the signal-mediated nuclear exit of mature viruses is a process that is temporally and mechanistically distinguishable from the nonspecific cellular release of empty capsids. Mutations in the CRM1 binding domain of NS2 that were naturally selected in mice showed, in synchronously infected 324K cells, that an NS2-CRM1 cytoplasmic interaction occurred several hours prior to a general increase in the nuclear release of viral antigens, mainly the NS1 major viral nonstructural protein lacking a recognizable conventional NES, and also of the empty capsid (35). In addition, the release of the capsid into the cytoplasm late in the infection is relatively slow, since it can be stained with an antibody (15, 35, 40), whereas the export of mature viruses and heated capsids from the nucleus to the cell surface proceeded rapidly, with no cytoplasmic accumulation by IF (Fig. 2 to 6). In summary, our data are consistent with previous reports of an effect on nuclear release of the MVM capsid induced by the NS2-CRM1 interaction (15, 40), which may also benefit the distinct 2Nt-mediated active transport of mature virions, although the role of CRM1 in both processes must be through an indirect phenomenon in which other pleiotropic properties of this cellular transporter may be involved (17, 75), and this phenomenon deserves further research.

Structural transitions during MVM trafficking across NPC. Based on this and previous reports, we propose an integrative model of the signals regulating MVM movement in and out of the mammalian nucleus, as shown in Fig. 7. At the initiation of the infection, the 2Nt termini exposed on the capsid surface of

the incoming virus are cleaved by cellular proteases during cytoplasmic uptake (8, 50), and thus their NES activity would not interfere with the subsequent process of nuclear entry. Subsequent stages of the entry process would facilitate a distortion of the capsid leading to the exposure of the NLSs placed at the VP1 N terminus, which are internal in the particle (10, 69) but are strictly required to initiate infection (33). It is still uncertain whether further disassembly of the small parvovirus particle is required to deliver the viral genome across the NPC, as probed for several larger viruses (12, 66, 73). Late in the infection, the mature MVM virions exit the nucleus in an apparently intact configuration (Fig. 7, left panel) in which the nuclear import sequences mapped in the structural proteins (32, 33, 69) are hidden in the capsid structure and thus would not compete with the export activity of 2Nt. As explained above, the degree of 2Nt phosphorylation would ultimately dictate the main nuclear export route accessed by the virions. Thus, intracellular structural transitions of the MVM capsid configuration may trigger an alternate exposed outside of the shell across the channel at the fivefold axis (1, 68) of the nuclear transport signals localized at the N termini of the VP protein subunits, driving the traffic of the virus through the NPC. In support of this model, mutations of the interfacial amino acid residues surrounding the base of the channel hampered MVMp infectivity (55).

The exposure of transport signals at flexible protein ends may be an advantageous structural solution evolved by metastable viral capsids to traverse across the central channel of the NPC. The function of 2Nt as the NES of a large nucleoprotein complex such as the approximately 25-nm-diameter MVM virus is consistent with the adapter-mediated highly efficient export of the large ribosomal subunit (67), which is a cargo of similar size. Although the upper limit for nondeformable cargo that can pass through the NPC channel is in the 25- to 39-nm range (14, 49), it is matter of speculation whether karyophilic viruses with larger sizes can gain facilitated transport out of the nucleus by alterations of the NPC protein composition induced during infection, as described for some cytoplasmic viruses (22). Active nuclear export prior to cell degeneration may allow viruses to evade apoptosis and other host defense mechanisms as well as facilitating spread among tissues, since the extensive cellular lysis frequently observed in cultures infected by cytolytic viruses may not largely develop if the integrity of the infected cell is protected within the architecture of the organs.

ACKNOWLEDGMENTS

We thank E. Izaurralde and W. Ansorge (EMBL, Heidelberg, Germany) for their respective laboratory support and use of a microinjection facility, Minoru Yoshida (University of Tokyo) for a generous supply of LMB, P. Tattersall (Yale, New Haven, Conn.) for the infectious molecular clone of MVMp, M. Fornerod (EMBL) for the α-hCRM-1 antibody, C. Parrish (Cornel, N.Y.) for the hybridoma producing the B7 capsid MAb, C. A. Astell (Columbia, Canada) for the anti-NS1 monoclonal antibody, P. Beard (SICR, Epalinges, Spain) for advice on the manuscript, and C. Sanchez (CBMSO, Madrid, Spain) for confocal microscopy support.

This work was supported by grants from the Spanish Ministry of Science and Technology (SAF2001-1325, CICYT) and Comunidad de Madrid (CAM 07B/0020/2002). The Centro de Biología Molecular Severo Ochoa is supported in part by an institutional grant from Fundación Ramón Areces. B.M. was supported by a postdoctoral fellowship of the CAM.

REFERENCES

1. **Agbandje-McKenna, M., A. LLamas-Saiz, F. Wang, P. Tattersall, and M. G. Rossmann.** 1998. Functional implications of the structure of the murine parvovirus minute virus of mice. Structure **6:**1369–1381.
2. **Boyle, W. J., P. van der Geer, and T. Hunter.** 1991. Phosphopeptide mapping and phosphoamino acid analysis by two-dimensional separation on thin-layer cellulose plates. Methods Enzymol. **201:**110–149.
3. **Brown, V. M., E. Y. Krynetski, N. F. Krynetskaia, D. Grieger, S. T. Mukatira, K. G. Murti, C. A. Slaughter, H.-W. Park, and W. E. Evans.** 2004. A novel crm1-mediated nuclear export signal governs nuclear accumulation of glyceraldehyde-3-phosphate dehydrogenase following genotoxic stress. J. Biol. Chem. **279:**5984–5992.
4. **Brownstein, D. G., A. L. Smith, R. O. Jacoby, E. A. Johnson, G. Hansen, and P. Tattersall.** 1991. Pathogenesis of infection with a virulent allotropic variant of minute virus of mice and regulation by host genotype. Lab. Investig. **65:**357–363.
5. **Caillet-Fauquet, P., M. Perros, A. Brandenburger, P. Spegelaere, and J. Rommelaere.** 1990. Programmed killing of human cells by means of an inducible clone of parvoviral genes encoding non-structural proteins. EMBO J. **9:**2989–2995.
6. **Carreira, A., M. Menéndez, J. Reguera, J. M. Almendral, and M. G. Mateu.** 2004. *In vitro* disassembly of a parvovirus capsid and effect on capsid stability of heterologous peptide insertions in surface loops. J. Biol. Chem. **279:**6517–6525.
7. **Clayson, E. T., L. V. Brandon, and R. W. Compans.** 1989. Release of simian virus 40 virions from epithelial cells is polarized and occurs without cell lysis. J. Virol. **63:**2278–2288.
8. **Cotmore, S. F., and P. Tattersall.** 1987. The autonomously replicating parvoviruses of vertebrates. Adv. Virus Res. **33:**91–173.
9. **Cotmore, S. F., A. M. D'Abramo, L. F. Carbonell, J. Bratton, and P. Tattersall.** 1997. The NS2 polypeptide of parvovirus MVM is required for capsid assembly in murine cells. Virology **231:**267–280.
10. **Cotmore, S. F., A. M. D'Abramo, C. M. Ticknor, and P. Tattersall.** 1999. Controlled conformational transitions in the MVM virions expose the VP1 N-terminus and viral genome without particle disassembly. Virology **254:** 169–181.
11. **Crawford, L. V.** 1966. A minute virus of mice. Virology **29:**605–612.
12. **Cullen, B. C.** 2001. Journey to the center of the cell. Cell **105:**697–700.
13. **Daigle, N., J. Beaudouin, L. Hartnell, G. Imrech, E. Hallberg, J. Lippincott-Schwartz, and J. Ellenberg.** 2001. Nuclear pore complexes form immobile networks and have a very low turnover in live mammalian cells. J. Cell Biol. **154:**71–84.
14. **Dworetzky, S. L., and C. M. Feldherr.** 1988. Translocation of RNA-coated gold particles through the nuclear pores of oocytes. J. Cell Biol. **106:**575–584.
15. **Eichwald, V., L. Daeffler, M. Klein, J. Rommelaere, and N. Salomé.** 2002. The NS2 proteins of parvovirus minute virus of mice are required for efficient nuclear egress of progeny virions in mouse cells. J. Virol. **76:**10307–10319.
16. **Fischer, U., J. Huber, W. C. Boelens, I. W. Mattaj, and R. Lührmann.** 1995. The HIV-1 Rev activation domain is a nuclear export signal that accesses an export pathway used by specific cellular RNAs. Cell **82:**475–483.
17. **Forgues, M., M. J. Difilippantonio, S. P. Linke, T. Ried, K. Nagashima, J. Feden, K. Valerie, K. Fukasawa, and X. W. Wang.** 2003. Involvement of Crm1 in hepatitis B virus X protein-induced aberrant centriole replication and abnormal mitotic spindles. Mol. Cell. Biol. **23:**5282–5292.
18. **Fornerod, M., M. Ohno, M. Yoshida., and I. W. Mattaj.** 1997. Crm1 is an export receptor for leucine-rich nuclear export signals. Cell **90:**1051–1060.
19. **Fukuda, M., S. Asano, T. Nakamura, M. Adachi, M. Yoshida, M. Yanagida, and E. Nishida.** 1997. CRM1 is responsible for intracellular transport mediated by the nuclear export signal. Nature **390:**308–311.
20. **Gallic, L. L., L. Virgilio, P. Cohen, B. Biteau, and G. Mavrothalassitis.** 2004. ERF nuclear shuttling, a continuous monitor of ERK activity that links it to cell cycle progression. Mol. Cell. Biol. **24:**1206–1218.
21. **Gardiner, E. M., and P. Tattersall.** 1988. Mapping of the fibrotropic and lymphotropic host range determinants of the parvovirus minute virus of mice. J. Virol. **62:**2605–2613.
22. **Gustin, K. E., and P. Sarnow.** 2001. Effects of poliovirus infection on nucleocytoplasmic trafficking and nuclear pore complex composition. EMBO J. **20:**240–249.
23. **Hernando, E., A. L. Llamas-Saiz, C. Foces-Foces, R. McKenna, L. Portman, M. Agbandje-McKenna, and J. M. Almendral.** 2000. Biochemical and physical characterization of parvovirus minute virus of mice virus-like particles. Virology **267:**299–309.
24. **Izaurralde, E.** 2002. Nuclear export of messenger RNA. Results Probl. Cell Differ. **35:**133–150.
25. **Kaffman, A., N. M. Rank, E. M. O'Neill, L. S. Huang, and E. K. O'Shea.** 1998. The receptor Msn5 exports the phosphorylated transcription factor Pho4 out of the nucleus. Nature **396:**482–486.

26. **Kalderon, D., B. L. Roberts, W. D. Richardson, and A. E. Smith.** 1984. A short amino acid sequence able to specify nuclear location. Cell **39:**499–509.
27. **Kann, M., B. Sodeik, A. Vlachou, W. H. Gerlich, and A. Helenius.** 1999. Phosphorylation-dependent binding of hepatitis B virus core particles to the nuclear pore complex. J. Cell Biol. **145:**45–55.
28. **Kudo, N., B. Wolff, T. Sekimoto, E. P. Schreiner, Y. Yoneda, M. Yanagida, S. Horinouchi, and M. Yoshida.** 1998. Leptomycin B inhibition of signal-mediated nuclear export by direct binding to CRM1. Exp. Cell Res. **242:**540–547.
29. **Kutay, U., F. R. Bichoff, S. Kostka, R. Kraft, and D. Gorlich.** 1997. Export of importin α from the nucleus is mediated by a specific nuclear transport factor. Cell **90:**1061–1071.
30. **Langeveld, J. P. M., J. L. Casal, C. Vela, K. Dalsgaard, S. H. Smale, W. C. Puijk, and R. H. Meloen.** 1993. B-cell epitopes of canine parvovirus: distribution on the primary structure and exposure on the viral surface. J. Virol. **67:**765–772.
31. **Lindsay, M. E., K. Plafker, A. E. Smith, B. E. Clurman, and I. G. Macara.** 2002. Npap60/Nup50 is a tri-stable switch that stimulates importin-α:β-mediated nuclear protein import. Cell **110:**349–360.
32. **Lombardo, E., J. C. Ramírez, M. Agbandje-Mckenna, and J. M. Almendral.** 2000. A β-stranded motif drives capsid protein oligomers of the parvovirus minute virus of mice into the nucleus for viral assembly. J. Virol. **74:**3804–3814.
33. **Lombardo, E., J. C. Ramírez, J. García, and J. M. Almendral.** 2002. Complementary roles of multiple nuclear targeting signals in the capsid proteins of the parvovirus minute virus of mice during assembly and onset of infection. J. Virol. **76:**7049–7059.
34. **López-Bueno, A., M. G. Mateu, and J. M. Almendral.** 2003. High mutant frequency in populations of a DNA virus allows evasion from antibody therapy in an immunodeficient host. J. Virol. **77:**2701–2708.
35. **López-Bueno, A., N. Valle, J. M. Gallego, J. Pérez, and J. M. Almendral.** 2004. Enhanced cytoplasmic sequestration of the nuclear export receptor CRM1 by NS2 mutations developed in the host regulates parvovirus fitness. J. Virol. **78:**10674–10684.
36. **Macara, I. G.** 2001. Transport into and out of the nucleus. Microbiol. Mol. Biol. Rev. **65:**570–594.
37. **Maroto, B., J. C. Ramírez, and J. M. Almendral.** 2000. Phosphorylation status of the parvovirus minute virus of mice particle: mapping and biological relevance of the major phosphorylation sites. J. Virol. **74:**10892–10902.
38. **Mattaj, I. W., and L. Englmeier.** 1998. Nucleocytoplasmic transport: the soluble phase. Annu. Rev. Biochem. **67:**265–306.
39. **Mettenleiter, T. C.** 2002. Herpesvirus assembly and egress. J. Virol. **76:**1537–1547.
40. **Miller, C. L., and D. J. Pintel.** 2002. Interaction between parvovirus NS2 protein and nuclear export factor Crm1 is important for viral egress from the nucleus of murine cells. J. Virol. **76:**3257–3266.
41. **Mousset, S., and J. Rommelaere.** 1982. Minute virus of mice inhibits cell transformation by simian virus 40. Nature (London) **300:**537–539.
42. **Muranyi, W., J. Haas, M. Wagner, G. Krohne, and U. H. Koszinowski.** 2002. Cytomegalovirus recruitment of cellular kinases to dissolve the nuclear lamina. Science **297:**854–857.
43. **Muzyczka, N., and K. I. Berns.** 2001. Parvoviridae: the viruses and their replication. *In* D. M. Knipe et al. (ed.), Fields virology. Lippincott Williams & Wilkins, Philadelphia, Pa.
44. **Nakanishi, A., D. Shum, H. Morioka, E. Otsuka, and H. Kasamatsu.** 2002. Interaction of the Vp3 nuclear localization signal with the importin α2/β heterodimer directs nuclear entry of infecting simian virus 40. J. Virol. **76:**9369–9377.
45. **Nakielny, S., and G. Dreyfuss.** 1999. Transport of proteins and RNAs in and out of the nucleus. Cell **99:**677–690.
46. **Ohno, M., A. Segref, A. Bachi, M. Wilm, and I. W. Mattaj.** 2000. PHAX, a mediator of UsnRNA nuclear export whose activity is regulated by phosphorylation. Cell **101:**187–198.
47. **O'Neill, R. E., J. Talon, and P. Palese.** 1998. The influenza virus NEP (NS2 protein) mediates the nuclear export of viral ribonucleoproteins. EMBO J. **17:**288–296.
48. **Ossareh-Nazari, B., F. Bachelerie, and C. Dargemont.** 1997. Evidence for a role of CRM1 in signal-mediated nuclear protein export. Science **278:**141–144.
49. **Panté, N., and M. Kann.** 2002. Nuclear pore complex is able to transport macromolecules with diameters of 39 nm. Mol. Biol. Cell **13:**425–434.
50. **Paradiso, P. R.** 1981. Infectious process of the parvovirus H-1: correlation of protein content, particle density, and viral infectivity. J. Virol. **39:**800–807.
51. **Paradiso, P. R., K. R. Williams, and R. L. Constantino.** 1984. Mapping of the amino terminus of the H-1 parvovirus major capsid protein. J. Virol. **52:**77–81.
52. **Puvion-Dutilleul, F., S. Besse, E. Pichard, and C. Cajean-Feroldi.** 1998. Release of viruses and viral DNA from the nucleus to cytoplasm of HeLa cells at late stages of productive adenovirus infection as revealed by electron microscope in situ hybridization. Biol. Cell **90:**5–38.
53. **Rabe, B., A. Vlachou, N. Panté, A. Helenius, and M. Kann.** 2003. Nuclear import of hepatitis B capsids and release of the viral genome. Proc. Natl. Acad. Sci. USA **100:**9849–9854.
54. **Ramírez, J. C., A. Fairén, and J. M. Almendral.** 1996. Parvovirus minute virus of mice strain i multiplication and pathogenesis in the newborn mouse brain is restricted to proliferative areas and to migratory cerebellar young neurons. J. Virol. **70:**8109–8116.
55. **Reguera, J., A. Carreira, L. Riolobos, J. M. Almendral, and M. G. Mateu.** 2004. Role of interfacial amino acid residues in assembly, stability, and conformation of a spherical virus capsid. Proc. Natl. Acad. Sci. USA **101:**2724–2729.
56. **Richards, S. A., K. L. Carey, and I. G. Macara.** 1997. Requirement of guanosine triphosphate-bound Ran for signal-mediated nuclear protein export. Science **276:**1842–1848.
57. **Robbins, J., S. M. Dilworth, R. A. Laskey, and C. Dingwall.** 1991. Two interdependent basic domains in nucleoplasmin nuclear targeting sequence: identification of a class of bipartite nuclear targeting sequence. Cell **64:**615–623.
58. **Ryan, K. J., and S. R. Wente.** 2000. The nuclear pore complex: a protein machine bridging the nucleus and cytoplasm. Curr. Opin. Cell Biol. **12:**361–371.
59. **Santarén, J. F., J. C. Ramírez, and J. M. Almendral.** 1993. Protein species of the parvovirus minute virus of mice strain MVMp: involvement of phosphorylated VP-2 subtypes in viral morphogenesis. J. Virol. **67:**5126–5138.
60. **Segovia, J. C., J. M. Gallego, J. A. Bueren, and J. M. Almendral.** 1999. Severe leukopenia and dysregulated erythropoiesis in SCID mice persistently infected by the parvovirus minute virus of mice. J. Virol. **73:**1774–1784.
61. **Stade, K., C. S. Ford, C. Guthrie, and K. Weis.** 1997. Exportin 1 (Crm1p) is an essential nuclear export factor. Cell **90:**1041–1050.
62. **Stuven, T., E. Hartmann, and D. Gorlich.** 2003. Exportin 6: a novel nuclear receptor that is specific for profilin-actin complexes. EMBO J. **22:**5928–5940.
63. **Tattersall, P., and J. Bratton.** 1983. Reciprocal productive and restrictive virus-cell interaction of immunosuppressive and prototype strains of minute virus of mice. J. Virol. **46:**944–955.
64. **Tattersall, P., P. J. Cawte, A. J. Shatkin, and D. C. Ward.** 1976. Three structural polypeptides coded for by minute virus of mice, a parvovirus. J. Virol. **20:**273–289.
65. **Tattersall, P., A. J. Shatkin, and D. C. Ward.** 1977. Sequence homology between the structural polypeptides of minute virus of mice. J. Mol. Biol. **111:**375–394.
66. **Trotman, L., N. Mosberger, M. Fornerod, R. Stidwill, and U. F. Greber.** 2001. Import of adenovirus DNA involves the nuclear pore complex receptor CAN/Nup214 and histone H1. Nat. Cell Biol. **3:**1092–1100.
67. **Trotta, C. R., E. Lund, L. Kahan, A. W. Johnson, and J. E. Dahlberg.** 2003. Coordinated nuclear export of 60S ribosomal subunits and NMD3 in vertebrates. EMBO J. **22:**2841–2851.
68. **Tsao, J., M. S. Chapman, M. Agbandje, W. Keller, K. Smith, H. Wu, M. Luo, T. J. Smith, M. G. Rossmann, R. W. Compans, and C. R. Parrish.** 1991. The three-dimensional structure of canine parvovirus and its functional implications. Science **251:**1456–1464.
69. **Vihinen-Ranta, M., D. Wang, W. S. Weichert, and C. R. Parrish.** 2002. The VP1 N-terminal sequence of canine parvovirus affects nuclear transport of capsids and efficient cell infection. J. Virol. **76:**1884–1891.
70. **Warner, J. R.** 1999. The economics of ribosome biosynthesis in yeast. Trends Biochem. Sci. **24:**437–441.
71. **Weigel, S., and M. Dobbelstein.** 2000. The nuclear export signals within the E4orf6 protein of adenovirus type 5 support virus replication and cytoplasmic accumulation of viral mRNA. J. Virol. **74:**764–772.
72. **Weis, K.** 2003. Regulating access to the genome: nucleocytoplasmic transport throughout the cell cycle. Cell **112:**441–451.
73. **Whittaker, G. R., M. Kann, and A. Helenius.** 2000. Viral entry into the nucleus. Annu. Rev. Cell Dev. Biol. **16:**627–651.
74. **Wolff, B., J. J. Sanglier, and Y. Wang.** 1997. Leptomycin B is an inhibitor of nuclear export: inhibition of nucleo-cytoplasmic translocation of the human immunodeficiency virus type 1 (HIV-1) Rev protein and Rev-dependent mRNA. Chem. Biol. **4:**139–147.
75. **Yamaguchi, R., and J. Newport.** 2003. A role for Ran-GTP and Crm1 in blocking re-replication. Cell **113:**115–125.